

# A Polychromatic Theory of Emission

Ivan Fernandez-Corbaton,<sup>1,\*</sup> Maxim Vavilin,<sup>2</sup> and Markus Nyman<sup>1</sup>

<sup>1</sup>*Institute of Nanotechnology, Karlsruhe Institute of Technology, Kaiserstr. 12, 76131 Karlsruhe, Germany*

<sup>2</sup>*Institut für Theoretische Festkörperphysik, Karlsruhe Institute of Technology, Kaiserstr. 12, 76131 Karlsruhe, Germany*

The control of thermal radiation by means of micro-structured materials is an active area of research with applications such as thermophotovoltaics and radiative cooling. The original theories of thermal radiation, derived for electromagnetically large objects, predict unpolarized, omnidirectional and uncorrelated radiation. Microstructures, however, exhibit thermal emissions that can be polarized, highly directional, and spatially and temporally correlated. The original theories are also restricted to thermal equilibrium situations. In particular, they do not apply to steady-state emissions of electromagnetically small objects under a stationary illumination, where one expects significant differences in the shape and number of photons of the illuminating and emitted spectra, much as what happens when an object is under the sun. In here, we establish a polychromatic framework to predict thermal radiation in the stationary regime, which includes thermal equilibrium. After identifying an object-dependent set of independent polychromatic absorption modes, we assume that the emission also occurs independently through the outgoing versions of each polychromatic mode. Energy conservation leads then to a Kirchhoff-like law *for each polychromatic mode*. The salient properties of the polychromatic theory are: Emission in frequencies absent in the illumination, change in the number of photons, and applicability to both thermal radiation and luminescence upon illumination with a continuous wave laser, as long as the emitted power depends linearly on the input intensity. These properties are independent of the chosen set of polychromatic modes. In this work, we chose the absorption modes derived from the scattering operator of a given object, and use the T-matrix formalism for computations, which applies to general objects, including microscopic ones. Some counter-intuitive results motivate the future search for a different set of modes.

It is possible to make ice at temperatures well above zero degrees. This was known by ancient civilizations in Persia and India, that made ice during some nights. We now understand that this is possible thanks to radiative cooling, which connects the water on the Earth surface to the ultracold outer space at  $-270^\circ\text{C}$  through the atmospheric transparency windows. This surprising possibility illustrates the potential benefits of controlling thermal radiation. However, it is already known that the most basic theories are insufficient for describing and engineering the thermal radiation properties of general objects. In the works of Kirchhoff and Planck [1, 2], the thermal equilibrium radiation is isotropic, unpolarized, and uncorrelated in space and time. Both of them used ray optics and assumed the objects under consideration and their features to be much larger than the wavelength [3][4, Chap. 4.7]. When such assumptions are not fulfilled, thermal radiation can be polarized [5, 6], and exhibit correlations in both space [7] and time [8, 9]. Modern fabrication techniques can structure materials at the sub-micrometer scale. Such systems break the traditional assumptions, allowing one to shape thermal emissions [10–12] in applications such as thermo-photovoltaic energy conversion and daytime radiative cooling [13, 14]. The beneficial complexity afforded by modern fabrication techniques has to be included in the theoretical models.

One of the cornerstones of thermal radiation theory is Kirchhoff law [2], which states that emissivity equals

absorptivity. In reciprocal systems in thermal equilibrium with the surrounding electromagnetic bath, Kirchhoff law of heat radiation equates the emission of a given frequency towards a certain direction with the absorption of the radiation of the same frequency coming towards the object along the opposite direction. Then, i) the rate of photons absorbed and emitted at any given frequency must be equal so that there is no net flux of energy, and ii) the frequency spectrum of the thermal radiation from the object is equal to the spectrum of the incoming bath modulated by the frequency- and direction-dependent absorption of the object. Rules i) and ii) are a consequence of treating each frequency independently. The radiation of heat, however, does not necessarily obey them. Consider objects under stationary illumination, that is, when the statistics of the incoming field do not change with time, and the emission and absorption rates are constant. Stationarity includes thermal equilibrium between the object and the radiation field, where both are at the same temperature. Stationarity also includes cases where the object is at a different temperature than its surroundings because of the effect of an external stationary illumination. A car under the sun, and the thermal radiation from Earth would be examples at large scales. In such examples, it is clear that the thermal radiation emitted by the object has a very different frequency content than the illuminating sun light, and that, when visible light is absorbed and infrared radiation is emitted energy conservation implies that the number of emitted photons must be larger than the number of absorbed photons. At much smaller scales, such pronounced frequency changes can be seen, for example in [15], where a micro-structured film

---

\* ivan.fernandez-corbaton@kit.edu

shifts the green sunlight onto the red band, which is useful for photosynthesis. Even in thermal equilibrium, the assumption that the frequency components of the emission spectra are uncorrelated can be questioned when the electromagnetic size of the objects violates the assumptions of the traditional theories. Such violation would be different from the correlations predicted in the thermal emission spectrum of time-varying systems where the material properties are explicitly modulated in time [16].

In here, we establish a polychromatic framework to quantitatively predict thermal radiation, where changes in the frequency spectrum and number of photons appear naturally. Given a suitable set of polychromatic modes, and, assuming stationary illumination, we formulate a Kirchhoff-like equation for each mode of the object in question: The rate of emission of photons through a given polychromatic mode is equal to the rate of energy absorption through such mode, divided by the energy of the mode. The modes of the object are known to be relevant for the accurate calculation of thermal radiation. For example, the surface waves of planar geometries create very large thermal energy densities near the surface [8, 9], and polaritons affect the transfer of heat in the near-field [17, 18]. In this work, we choose the polychromatic modes that can be derived from the T-matrix. The T-matrix [19] is a popular and powerful approach in theoretical nanophotonics [20, 21], that can be applied to macroscopic objects and also to molecules [22, 23]. While there exist theories of thermal radiation whose formalism can be readily connected to modes derived from the T-matrix [24–26], they do not cover the potential re-distribution of the frequency content, which we are able to do thanks to the recent reformulation of the monochromatic T-matrix formalism [27], onto an inherently polychromatic one [28]. Rather independently of the chosen set of modes, the polychromatic character of the theory endows it with two inherent related properties that are desirable for modeling emission: The emission at frequencies that are not present in the illumination, and the change in the number of photons by emission rates that are higher or lower than absorption rates. The change in the number of photons is a consequence of energy conservation, for example, when high-energy photons are absorbed but many more low-energy photons emitted. The ability to radiate frequencies that are not present in the illumination is because a polychromatic mode will absorb an incident field that has at least some spectral overlap with it, but will always emit in the whole spectrum of the mode. Different choices of polychromatic modes result in different predictions of the emission spectra, opening the question of which is the most suitable set of modes. We also note that emission in frequencies that the illumination does not contain is also a hallmark of luminescence. The polychromatic formalism can thus accommodate both thermal radiation and luminescence upon pumping by a narrowband continuous wave laser, because both cases are stationary. We note that there already exist methods that connect thermal

radiation and luminescence [29, 30].

The rest of the article is organized as follows. In Sec. I, we use the polychromatic T-matrix to identify a set of polychromatic absorption modes. The polychromatic absorption modes define independent channels of absorption. An illumination containing a single such mode cannot be absorbed by any other mode. In Sec. II, we devise a theory of emission based on two assumptions. First, that the emission will occur through the radiating versions of the polychromatic absorption modes, and second, that, in the stationary regime, the rate of energy absorption per mode is equal to the rate of energy emission per mode. The assumptions lead to a polychromatic Kirchhoff-like equation for each mode. The thermal spectrum of a given object can be computed using such equations. Section III contains formulas for when a generic thermal bath surrounds the object, and their particularization to a Planckian bath. The emission spectra from the object obtained using this polychromatic approach differs from the emission spectra obtained with the more common approach where the modes of absorption/emission are taken to be monochromatic. Both predictions converge to each other as the polychromatic modes become more and more narrowband around a given central frequency. The formulas from Sec. III are applied in Sec. IV to the case of achiral spheres, and predictions of their absolute thermal spectra in photons per wavenumber are shown.

The polychromatic modes chosen in this article can be readily obtained from the polychromatic T-matrix that, in turn, can be readily obtained from the usual monochromatic T-matrices [28, Eq. 113], computed for many frequencies in the spectral range of interest. Many publicly available codes exist for computing monochromatic T-matrices [31–33], and for using T-matrices to obtain the response of periodic arrays such as metasurfaces [34–36]. All the necessary elements for computing predictions with both the monochromatic and polychromatic theories are hence already available. This facilitates the experimental testing of the polychromatic theory.

The choice of polychromatic modes made in Sec. I produces counter-intuitive outcomes in the high energy region of the spectrum. This indicates the potential inadequacy of this particular set of modes, and motivates the search for an alternative set. We highlight that the salient properties of the polychromatic theory are independent of the choice of polychromatic modes: Namely the emission in frequencies absent in the illumination, the change in the number of photons, and the applicability to both thermal radiation and stationary luminescence processes that are linear with the input intensity. Section V concludes the article with the final discussions and outlook.

## I. THE POLYCHROMATIC ABSORPTION MODES

The T-matrix, or transfer operator T is related to the scattering operator S as<sup>1</sup>:

$$S = I + T, \quad (1)$$

where I is the identity operator. The scattering operator S of a material system acts on incoming illumination fields to produce the corresponding outgoing fields. Appendix A summarizes the mathematical setting that we use in this article, which is based on the Hilbert space of solutions of Maxwell equations  $\mathbb{M}$ . We adopt the bracket notation by Dirac, and denote a particular solution of Maxwell equations as  $|f\rangle$ . Notably, the projection of a field  $|f\rangle$  onto itself,  $\langle f|f\rangle$ , is equal to the number of photons in the field [37].

The absorption by the object can be formalized by considering the difference between the number of photons of the incoming field  $|f\rangle$ , and the outgoing field  $S|f\rangle$ :

$$\langle f|f\rangle - \langle f|S^\dagger S|f\rangle = \langle f|I - S^\dagger S|f\rangle = \langle f|Q|f\rangle, \quad (2)$$

where the last equality is the definition of the operator Q, which, as a function of T can be written as

$$Q = I - S^\dagger S = -T - T^\dagger - T^\dagger T. \quad (3)$$

The operator Q has the following singular value decomposition (see App. A 1):

$$Q = \sum_s q_s^2 |s\rangle\langle s| = \sum_s |\hat{s}\rangle\langle \hat{s}| = \sum_s P_s, \quad (4)$$

where the third and fourth equalities are the definition of the modes  $|\hat{s}\rangle = q_s |s\rangle$ , and operators  $P_s$ , respectively. The left and right singular vectors are equal in this case because Q is self-adjoint,  $Q = Q^\dagger$ , and we further assume that it is positive semi-definite, that is  $\langle f|Q|f\rangle \geq 0$ . The latter assumption implies that the object does not have gain. The set of singular vectors  $|s\rangle$  is an orthonormal basis in  $\mathbb{M}$ :  $\langle u|s\rangle = \delta_{us}$ , where  $\delta_{us}$  is the Kronecker delta. We call them *polychromatic absorption modes*.

Let us now consider an incoming field proportional to one of the  $|s\rangle$  modes:  $|f\rangle = \alpha|s\rangle$ , where  $\alpha$  is a complex number. Upon light-matter interaction the illumination will be absorbed with efficiency  $q_s^2$ :

$$\frac{\langle f|Q|f\rangle}{\langle f|f\rangle} = \frac{|\alpha|^2 \langle s|Q|s\rangle}{|\alpha|^2} \stackrel{\text{Eq. (4)}}{=} q_s^2 \leq 1. \quad (5)$$

In this setting, a black body is characterized by a Q operator where  $q_s^2 = 1$  for all  $s$ , that is, a perfect absorber.

We highlight that the polychromatic absorption modes  $|s\rangle$  can potentially span the entire spectrum, as is also the case for Lorentzian lineshapes.

## II. EMISSION IN THE STATIONARY REGIME

In the scattering process the incoming field  $|f\rangle$  interacts with the object and produces the outgoing field  $S|f\rangle$ . Additionally, there can be a different kind of outgoing radiation emitted from the object, which we call emission. It is well-known that the absorption of electromagnetic energy by an object can lead to its subsequent emission. In this section, we devise a theory of emission using the polychromatic absorption modes.

We want to restrict ourselves to the case in which the system is stationary in the sense that the absorption and emission rates do not depend on time. In such regime, the scattering, emission, and absorption processes occur continuously. Since they last forever, the number of photons involved is not finite. This poses an obstacle because the formalism of Hilbert spaces assumes that the norms of the kets are finite. Such obstacle can be circumvented by defining a finite period of time  $t_p$ , and considering what happens only during such period. The amount of photons that interact with or are emitted by the object is then finite.

Let us denote by  $|f\rangle^{\text{in}}$  the incoming illumination field. Then,

$$\gamma_s^{\text{abs}} = \frac{\text{in}\langle f|P_s|f\rangle^{\text{in}}}{t_p} = \frac{q_s^2 |\langle s|f\rangle^{\text{in}}|^2}{t_p}, \quad (6)$$

is the rate of photon absorption through mode  $|s\rangle$ . In the stationary regime, and as long as  $t_p$  is long enough, the results for a given period  $t_p$  can be taken as valid for any period of time with length equal to  $t_p$ . We take  $t_p = 1$  second for convenience, since then the number of photons is directly equal to the rate of photons per second.

The total rate of energy absorption  $\beta^{\text{abs}}$  can also be decomposed as a sum over  $s$ :

$$\beta^{\text{abs}} = \text{in}\langle f|\frac{QH + HQ}{2}|f\rangle^{\text{in}} \stackrel{\text{Eq. (4)}}{=} \sum_s \text{in}\langle f|\frac{P_s H + H P_s}{2}|f\rangle^{\text{in}} \quad (7)$$

, where the first equality uses [38, Eq. (13)], and H is the energy operator, whose action on monochromatic fields is their multiplication by  $\hbar c_0 k$ , where  $\hbar$  is the reduced Planck constant,  $c_0$  the speed of light, and  $k$  the wavenumber.

Each of the polychromatic absorption modes can be turned into a polychromatic emission mode by changing its original incoming character into an outgoing one. Mathematically, this can be achieved by expressing the absorption modes in a basis of multipolar fields, and then changing the kind of spherical Hankel functions [39, Sec. 1].

We now assume that the emission from the object happens through such outgoing modes. That is, any photon emitted by the object is emitted in a single polychromatic  $|s\rangle^{\text{out}}$  mode. Furthermore, while in the stationary regime, we assume that, for each  $s$ , the rate of energy absorption is equal to the rate of energy emission. So,

<sup>1</sup> The difference from the common definition  $S = I+2T$  is explained in [28, Sec. 3].

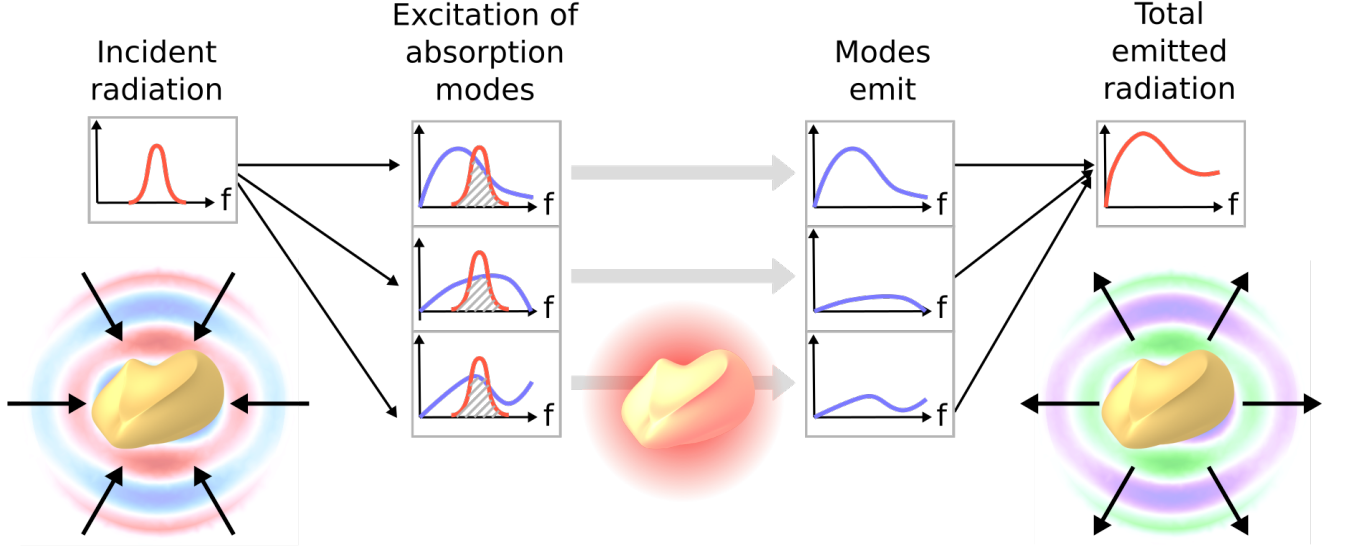


FIG. 1. Conceptual illustration of the calculation procedure. An incident field with a known spectrum is decomposed into the polychromatic absorption modes of the object, each of which absorb a fraction of the incident power. After absorption, the object stores the energy, and through internal conversion processes, all coherence between the initial fields is lost. The object then emits the absorbed power in such a way that the absorbed and emitted powers are equal for each mode separately. Adding up the results gives the total emission spectrum of the object.

there is zero energy flux for each individual  $s$  subspace. These are main assumptions the polychromatic theory of emission, and they would be the same for any other set of polychromatic modes.

According to the first of our assumptions, the total emission is composed by the modal emissions through the outgoing versions of the  $|s\rangle$  modes

$$|e\rangle^{\text{out}} = \sum_s e_s |s\rangle^{\text{out}}. \quad (8)$$

The rate of energy emission through mode  $s$  is the product of the energy of the mode [Eq. (A9) in App. A] and the photon emission rate  $\gamma_s^{\text{emi}}$ :

$$\beta_s^{\text{emi}} = {}^{\text{out}}\langle s|\mathbf{H}|s\rangle^{\text{out}} \gamma_s^{\text{emi}}. \quad (9)$$

According to our second assumption, the photon emission rate can be obtained from the zero energy flux condition as:

$$\beta_s^{\text{abs}} = \beta_s^{\text{emi}} \implies \gamma_s^{\text{emi}} = \frac{1}{2} \frac{{}^{\text{in}}\langle f|\mathbf{P}_s\mathbf{H} + \mathbf{H}\mathbf{P}_s|f\rangle^{\text{in}}}{{}^{\text{out}}\langle s|\mathbf{H}|s\rangle^{\text{out}}}. \quad (10)$$

Equations (8) and (10) imply one of the main differences between the polychromatic theory and many typical monochromatic approaches: The emission can contain frequency components that are not present in the illumination  $|f\rangle^{\text{in}}$ . This can be seen as follows. Each of the  $|s\rangle$  is polychromatic, and is pumped by  $|f\rangle^{\text{in}}$  with efficiency  $q_s^2 |\langle s|f\rangle^{\text{in}}|^2$ . Such efficiency can be non-zero as long as there is some overlap between the spectrum of

$|f\rangle^{\text{in}}$  and the spectrum of  $|s\rangle$ . After pumping, the emission in  $|s\rangle^{\text{out}}$  will contain all the frequency components of the mode, independently of whether such components were present in  $|f\rangle^{\text{in}}$  or not.

The potentially different rates of photon emission and absorption in Eq. (10) is another important difference with respect to monochromatic approaches. To illustrate this difference, let us consider a quasi-monochromatic incident field such that  $\mathbf{H}|f\rangle^{\text{in}} \approx \hbar c_0 k_0 |f\rangle^{\text{in}}$ , with which Eq. (10) becomes:

$$\gamma_s^{\text{emi}} \approx \frac{{}^{\text{in}}\langle f|\mathbf{P}_s|f\rangle^{\text{in}}}{{}^{\text{out}}\langle s|\mathbf{H}|s\rangle^{\text{out}}} \stackrel{\text{Eq. (6)}}{=} \gamma_s^{\text{abs}} \frac{\hbar c_0 k_0}{{}^{\text{out}}\langle s|\mathbf{H}|s\rangle^{\text{out}}}, \quad (11)$$

which says that when the energy of the  $|s\rangle^{\text{out}}$  mode is larger than the energy corresponding to the frequency of the illumination per photon, the object will emit less photons than it will absorb, and vice-versa. In monochromatic approaches, where emission and absorption are considered independently at each frequency, the photon emission and absorption rates need to be the same to avoid a net energy flux.

Since we want to be able to treat thermal radiation, we need to consider non-deterministic fields. We will denote by  $|\Psi_{\text{bath}}\rangle^{\text{in}}$  the random field impinging on the object, and by  $|\Phi_{\text{thermal}}\rangle^{\text{out}}$  the random emission from the object, which, according to Eq. (8) can be written as:

$$|\Phi_{\text{thermal}}\rangle^{\text{out}} = \sum_s \phi_s |s\rangle^{\text{out}}. \quad (12)$$

The  $\phi_s$  in Eq. (12) are complex random variables. We

will further assume that they have zero mean, and that they are uncorrelated to each other. Namely, their first and second moments are:

$$\mathbb{E}\{\phi_s\} = 0 \text{ for all } s, \text{ and } \mathbb{E}\{\phi_p^* \phi_s\} = \delta_{ps} \gamma_s^{\text{abs}}, \quad (13)$$

where  $\mathbb{E}\{\cdot\}$  denotes the statistical expected value. Equation (13) reflect the assumption that any given photon in the thermal radiation from the object is emitted in one of the  $|s\rangle^{\text{out}}$  modes. As a consequence, the thermal spectrum due to the object would, in general, be neither isotropic, nor uncorrelated in frequency, nor equally distributed in polarization.

At this point, we would use Eq. (10), except that it needs to be adapted for non-deterministic fields:

$$\boxed{\gamma_s^{\text{emi}} = \frac{1}{2} \frac{\mathbb{E}\{\langle \Psi_{\text{bath}} | P_s H + H P_s | \Psi_{\text{bath}} \rangle^{\text{in}}\}}{\text{out} \langle s | H | s \rangle^{\text{out}}}}. \quad (14)$$

Finally, we assume a complete loss of coherence between the incoming and the emitted fields. The assumptions that we have made in this section can be seen as analogous to those involved in Kirchhoff law, but using polychromatic absorption and emission modes instead of monochromatic plane waves [40, Eq. (2.18)], or monochromatic modes [26].

Equation (14) is the analogous to Kirchhoff law of thermal radiation in the polychromatic setting: It links the emission from a mode to the absorption of the bath by the incoming version of the same mode. It is important to note that Eq. (14) can be applied to any stationary bath, that is, in effect, it can be applied to any stationary field, including continuous wave lasers, or the superposition of a thermal bath and a continuous wave laser. It can also be applied to obtain the thermal emission spectrum of an object that is kept at some fixed temperature  $T$  by, for example, a warm plate. To such end, one further assumes that the thermal emission spectrum is independent of the environment. This assumption is used often and was already made by Kirchhoff (see [3, § 2]). Then, the desired spectrum can be computed by assuming that, instead of being heated by a plate, the object is immersed in, and in thermal equilibrium with, a Planckian radiation bath at temperature  $T$ . We will use this computational strategy in the next section.

Figure 1 illustrates the calculation procedure that we have just introduced. Knowing the incident field (e.g., the Planckian thermal bath), we calculate how much of it is absorbed in each of the polychromatic absorption modes. Internal conversion processes inside the object ensure that coherence with the incident field is lost. Then, each of the modes emits as much power as goes into it, and the total emission spectrum is the sum of the contributions from each mode.

### III. THERMAL SPECTRUM OF AN OBJECT AT TEMPERATURE $T$

We start by considering a general  $|\Psi_{\text{bath}}\rangle^{\text{in}}$ , and then restrict it to the Planckian distribution. Let us consider the plane wave expansion of  $|\Psi_{\text{bath}}\rangle^{\text{in}}$  (see App. A):

$$|\Psi_{\text{bath}}\rangle^{\text{in}} = \sum_{\lambda=\pm 1} \int_{\mathbb{R}^3} \frac{d^3\mathbf{k}}{k} \psi_{\lambda}(\mathbf{k}) |\mathbf{k}\lambda\rangle, \quad (15)$$

where  $k = |\mathbf{k}|$ ,  $|\mathbf{k}\lambda\rangle$  are plane waves of wavevector  $\mathbf{k}$  and helicity  $\lambda = 1$  or  $\lambda = -1$ , which correspond to left- and right-handed circular polarizations, respectively. Then

$$\begin{aligned} \frac{1}{2} \mathbb{E}\{\langle \Psi_{\text{bath}} | P_s H + H P_s | \Psi_{\text{bath}} \rangle^{\text{in}}\} = \\ \sum_{\lambda, \bar{\lambda}} \int_{\mathbb{R}^3} \frac{d^3\mathbf{k}}{k} \int_{\mathbb{R}^3} \frac{d^3\mathbf{q}}{q} \langle \bar{\lambda} \mathbf{q} | P_s | \mathbf{k} \lambda \rangle \frac{\hbar c_0 (k+q)}{2} \mathbb{E}\{\psi_{\lambda}(\mathbf{k}) \psi_{\bar{\lambda}}^*(\mathbf{q})\}, \end{aligned} \quad (16)$$

can be readily reached using that  $H|\mathbf{k}\lambda\rangle = \hbar c_0 k |\mathbf{k}\lambda\rangle$ .

Equation (16) can be used for a generic bath, that is, for a bath with any correlation  $\mathbb{E}\{\psi_{\lambda}(\mathbf{k}) \psi_{\bar{\lambda}}^*(\mathbf{q})\}$ . We now assume that the components of the thermal bath are uncorrelated in frequency, direction and polarization, and we also assume isotropy:

$$\mathbb{E}\{\psi_{\lambda}(\mathbf{k}) \psi_{\bar{\lambda}}^*(\mathbf{q})\} = \delta_{\lambda\bar{\lambda}} \delta(\mathbf{k} - \mathbf{q}) k^3 \mathbb{E}\{|\psi_{\lambda}(k)|^2\}, \quad (17)$$

where the  $k^3$  factor compensates the units of the Dirac delta  $\delta(\mathbf{k} - \mathbf{q})$ , which are always the inverse units of its argument, so that the left hand side of Eq. (17) and the last term in its right hand side have the same units, as it must be. Another way to validate Eq. (17) is by taking the expected value of  $\mathbb{E}\{\psi_{\lambda}(\mathbf{k}) \psi_{\bar{\lambda}}^*(\mathbf{q})\}$  in Eq. (B1) *before* using the orthogonality of the plane waves, and obtaining the same result for the average number of photons of  $|\Psi_{\text{bath}}\rangle^{\text{in}}$  as when such orthogonality is used first.

After substituting Eq. (17) into Eq. (16), we obtain:

$$\begin{aligned} \frac{1}{2} \mathbb{E}\{\langle \Psi_{\text{bath}} | P_s H + H P_s | \Psi_{\text{bath}} \rangle^{\text{in}}\} = \\ \sum_{\lambda=\pm 1} \int_{\mathbb{R}^3} \frac{d^3\mathbf{k}}{k} \mathbb{E}\{|\psi_{\lambda}(k)|^2\} k^2 \langle \lambda \mathbf{k} | P_s | \mathbf{k} \lambda \rangle \hbar c_0 k. \end{aligned} \quad (18)$$

We can now exploit the direction independence of  $\mathbb{E}\{|\psi_{\lambda}(k)|^2\}$  and split the radial and angular parts of

the  $\int_{\mathbb{R}^3} d^3\mathbf{k}$  integral<sup>2</sup> to arrive at:

$$\begin{aligned} & \frac{1}{2} \mathbb{E} \left\{ \text{in} \langle \Psi_{\text{bath}} | P_s H + H P_s | \Psi_{\text{bath}} \rangle^{\text{in}} \right\} = \\ & \sum_{\lambda=\pm 1} \int_{>0}^{\infty} dk \ k^3 (\hbar c_0 k) \mathbb{E} \left\{ |\psi_{\lambda}(k)|^2 \right\} \int d\hat{\mathbf{k}} \langle \lambda \mathbf{k} | P_s | \mathbf{k} \lambda \rangle \\ & \sum_{\lambda=\pm 1} \int_{>0}^{\infty} dk \ k^3 (\hbar c_0 k) \mathbb{E} \left\{ |\psi_{\lambda}(k)|^2 \right\} \int d\hat{\mathbf{k}} |\langle \lambda \mathbf{k} | \hat{s} \rangle|^2, \end{aligned} \quad (19)$$

where we make use  $|\hat{s}\rangle \langle \hat{s}| = P_s$  in the last line.

The value of  $\mathbb{E} \left\{ |\psi_{\lambda}(k)|^2 \right\}$  is the last piece of information needed to fully characterize the thermal spectrum of the object. The Planck spectrum is obtained by setting (see App. B):

$$\mathbb{E} \left\{ |\psi_{\lambda}(k)|^2 \right\} = \frac{Ac_0 k}{4\pi^2 \left( \exp\left(\frac{\hbar c_0 k}{k_B T}\right) - 1 \right)}, \quad (20)$$

where  $A$  is the surface area of the smallest sphere that encloses the object.

We are finally able to write down the expression for the rate of emission through a given mode:

$$\begin{aligned} \gamma_s^{\text{emi}} &= \frac{1}{2} \frac{\mathbb{E} \left\{ \text{in} \langle \Psi_{\text{bath}} | P_s H + H P_s | \Psi_{\text{bath}} \rangle^{\text{in}} \right\}}{\text{out} \langle s | H | s \rangle^{\text{out}}} \stackrel{\text{Eq. (19)}}{=} \\ & \frac{\sum_{\lambda=\pm 1} \int_{>0}^{\infty} dk \ \frac{Ac_0 k^4 (\hbar c_0 k)}{4\pi^2 \left( \exp\left(\frac{\hbar c_0 k}{k_B T}\right) - 1 \right)} \int d\hat{\mathbf{k}} |\langle \lambda \mathbf{k} | \hat{s} \rangle|^2}{\text{out} \langle s | H | s \rangle^{\text{out}}} = \\ & \frac{\sum_{\lambda=\pm 1} \int_{>0}^{\infty} dk \ \frac{Ac_0 k^4 (\hbar c_0 k)}{4\pi^2 \left( \exp\left(\frac{\hbar c_0 k}{k_B T}\right) - 1 \right)} \sum_{j=1}^{\infty} \sum_{m=-j}^j |\langle \lambda m j k | \hat{s} \rangle|^2}{\text{out} \langle s | H | s \rangle^{\text{out}}} \end{aligned} \quad (21)$$

, where the last equality readily follows from [28, Eq. (42)] and [41, Eq. (A12)], and the  $|kjm\lambda\rangle$  are multipolar fields of well-defined helicity. The label  $j = 1, 2, \dots$  is the multipolar order with  $j = 1$  corresponding to dipoles,  $j = 2$  to quadrupoles, and so on,  $m = -j \dots j$  is the component of the angular momentum in the  $z$  direction, and  $\lambda = \pm 1$  is the helicity (see App. A for more explicit expressions of the multipolar fields).

The emitted  $|\Phi_{\text{thermal}}\rangle^{\text{out}}$  is now fully characterized by the values of  $\gamma_s^{\text{emi}}$ . For example, we can compute its

angular spectrum as:

$$\begin{aligned} & \mathbb{E} \left\{ |\langle \lambda \mathbf{k} | \Phi_{\text{thermal}} \rangle^{\text{out}}|^2 \right\} = \\ & \mathbb{E} \left\{ \left| \sum_s \phi_s \langle \lambda \mathbf{k} | s \rangle^{\text{out}} \right|^2 \right\} \stackrel{\text{Eq. (13)}}{=} \sum_s \gamma_s^{\text{emi}} |\langle \lambda \mathbf{k} | s \rangle^{\text{out}}|^2 = \sum_s \\ & \frac{\sum_{\bar{\lambda}=\pm 1} \int_{>0}^{\infty} \frac{dq \ Ac_0 q^4 (\hbar c_0 q)}{4\pi^2 \left( \exp\left(\frac{\hbar c_0 q}{k_B T}\right) - 1 \right)} \sum_{j=1}^{\infty} \sum_{m=-j}^j |\langle \bar{\lambda} m j q | \hat{s} \rangle|^2}{\text{out} \langle \hat{s} | H | \hat{s} \rangle^{\text{out}}} |\langle \lambda \mathbf{k} | \hat{s} \rangle^{\text{out}}|^2 \\ & = \sum_s \frac{\sum_{\bar{\lambda}=\pm 1} \int_{>0}^{\infty} \frac{dq \ Ac_0 q^4 (\hbar c_0 q)}{4\pi^2 \left( \exp\left(\frac{\hbar c_0 q}{k_B T}\right) - 1 \right)} \int d\hat{\mathbf{q}} |\langle \bar{\lambda} \mathbf{q} | \hat{s} \rangle|^2}{\text{out} \langle \hat{s} | H | \hat{s} \rangle^{\text{out}}} |\langle \lambda \mathbf{k} | \hat{s} \rangle^{\text{out}}|^2, \end{aligned} \quad (22)$$

where we use  $|\hat{s}\rangle$  instead of  $|s\rangle$  in the  $\text{out} \langle \hat{s} | H | \hat{s} \rangle^{\text{out}}$  and  $|\langle \lambda \mathbf{k} | \hat{s} \rangle^{\text{out}}|^2$  for later convenience.

We will later compare predictions obtained with the polychromatic modes to those obtained with a typical way of computing the thermal angular spectrum using monochromatic plane waves: The directional Kirchhoff law [40, Eq. (2.18)]. It assumes the object to be electromagnetically reciprocal and, in our notation, reads (see App. C):

$$\begin{aligned} & \mathbb{E} \left\{ |\langle \lambda \mathbf{k} | \Phi_{\text{thermal}} \rangle^{\text{out}}|^2 \right\} = \\ & p_{\text{abs}}(|-\mathbf{k}\lambda\rangle) \mathbb{E} \left\{ |\langle \lambda - \mathbf{k} | \Psi_{\text{bath}} \rangle^{\text{in}}|^2 \right\} = \\ & \sum_s |\langle \lambda - \mathbf{k} | \hat{s} \rangle|^2 \left[ \frac{Ac_0 k^3}{4\pi^2 \left( \exp\left(\frac{\hbar c_0 k}{k_B T}\right) - 1 \right)} \right], \end{aligned} \quad (23)$$

where  $p_{\text{abs}}(|-\mathbf{k}\lambda\rangle)$  is the absorption probability upon illumination with the  $|-\mathbf{k}\lambda\rangle$  plane wave. The directional Kirchhoff law may be understood as returning towards the  $\mathbf{k}$  direction all the photons that have been absorbed coming from the opposite direction  $-\mathbf{k}$ . The number of photons is thereby preserved, in contrast to the polychromatic method. The energy is preserved in the monochromatic approach because each absorbed monochromatic photon with frequency  $c_0 k$  results in an emission of the same frequency.

According to Eq. (22) and Eq. (23), the polychromatic and monochromatic approaches produce different predictions. It is reassuring that the two methods coincide in the limit where the linewidths of all the  $|s\rangle$  modes tend to zero around the same central frequency (see App. C 1).

#### IV. NON-FREQUENCY COUPLING OBJECTS. APPLICATION TO SPHERES.

While the polychromatic T operator can in general couple together different frequency components of the incident field, we will assume here that it does not. Then, using Eq. (3), and the conventions from [28], one can arrive at the following expression for the Q operator in the

<sup>2</sup>  $\int d^3\mathbf{k} \equiv \int dk \ k^2 \int_{-1}^1 d(\cos\theta) \int_{-\pi}^{\pi} d\phi$ , where  $\theta$  and  $\phi$  are the polar and azimuthal angles of  $\mathbf{k}$  in spherical coordinates, respectively, and the shorthand notation  $\int d\hat{\mathbf{k}} \equiv \int_{-1}^1 d(\cos\theta) \int_{-\pi}^{\pi} d\phi$  will be used.

basis of electromagnetic multipolar fields:

$$-Q = \sum_{jm\lambda} \sum_{\bar{j}\bar{m}\bar{\lambda}} \int_{>0}^{\infty} dk k |kjm\lambda\rangle \langle \bar{\lambda}\bar{m}\bar{j}k| \left[ 2\tilde{T}_{\bar{j}\bar{m}\bar{\lambda}}^{jm\lambda}(k) + 2\left(\tilde{T}_{jm\lambda}^{\bar{j}\bar{m}\bar{\lambda}}(k)\right)^* + 4\sum_{\hat{j}\hat{m}\hat{\lambda}} \left(\tilde{T}_{jm\lambda}^{\hat{j}\hat{m}\hat{\lambda}}(k)\right)^* \tilde{T}_{\bar{j}\bar{m}\bar{\lambda}}^{\hat{j}\hat{m}\hat{\lambda}}(k) \right] \quad (24)$$

, where  $\tilde{T}_{\bar{j}\bar{m}\bar{\lambda}}^{jm\lambda}(k)$  are the matrix elements of the typical monochromatic T-matrices [28, Sec. 3.1]. The matrix form of the terms inside the square brackets in Eq. (24) is:

$$2\tilde{T}(k) + 2\tilde{T}^\dagger(k) + 4\tilde{T}^\dagger(k)\tilde{T}(k) = -\tilde{Q}(k), \quad (25)$$

where the  $(\bar{j}\bar{m}\bar{\lambda})$  labels index the columns, and the  $(jm\lambda)$  labels index the rows.

In computer calculations, the size of  $\underline{Q}(k)$  needs to be finite. For example, it is typical to ignore all the terms of multipolar order higher than some chosen  $j_{\max}$ . The cutoff must ensure that the terms that are left out do not contribute significantly to the results. Similarly, the  $k$  variable shall be discretized with a fine enough step.

We perform the singular value decomposition at each  $k$ :

$$\underline{Q}(k) = \sum_s \tilde{q}_s^2(k) \tilde{s}(k) \tilde{s}^\dagger(k), \text{ with } \tilde{s}^\dagger(k) \tilde{u}(k) = \delta_{su}, \quad (26)$$

where  $\tilde{s}(k)$  are the singular vectors, and use it to write  $\underline{Q}$  in Eq. (24) as:

$$Q = \sum_s \sum_{jm\lambda, \bar{j}\bar{m}\bar{\lambda}} \int_{>0}^{\infty} dk k |kjm\lambda\rangle \langle \bar{\lambda}\bar{m}\bar{j}k| \tilde{q}_s^2(k) [\tilde{s}(k)]_{jm\lambda} [\tilde{s}^\dagger(k)]_{\bar{j}\bar{m}\bar{\lambda}} = \sum_s P_s, \quad (27)$$

where the last equality defines the  $P_s$  for the case of non-frequency coupling objects. The orthogonality of the  $\tilde{s}(k)$  implies that  $(P_s)^\dagger (P_u) = 0$  unless  $s = u$ , and hence that the  $P_s$  operators define orthogonal subspaces.

While the  $P_s$  in Eq. (27) define independent absorption channels, as in Eq. (4), the situation is different because the  $P_s$  in Eq. (27) cannot be written as  $|\hat{s}\rangle\langle\hat{s}|$  for polychromatic  $|\hat{s}\rangle$ , because  $|\hat{s}\rangle\langle\hat{s}|$  mixes frequencies. It is however possible to still define polychromatic  $|\hat{s}\rangle$  modes that, for our purposes, can be used as those in Eq. (4), as long as the illumination is uncorrelated in frequency (App. D). The definition of such modes is:

$$|\hat{s}\rangle = \sum_{jm\lambda} \int_{>0}^{\infty} dk k \frac{\tilde{q}_s(k)}{k} [\tilde{s}(k)]_{jm\lambda} |kjm\lambda\rangle, \quad (28)$$

, where  $\int_{>0}^{\infty} dk k$  is the correct integration measure in the polychromatic setting [28], and  $[\tilde{s}(k)]_{jm\lambda}$  is the element of  $\tilde{s}(k)$  corresponding to given  $(jm\lambda)$  labels. Each  $|\hat{s}\rangle$  can potentially span the entire spectrum, and the monochromatic singular vectors  $\tilde{s}(k)$  that contribute to a particular  $|\hat{s}\rangle$  change smoothly with  $k$ . Such smoothness allows one to track the singular vectors across frequencies [42, Sec. III].

There are several reasons for the definition in Eq. (28). One is that, when computing the norm squared of  $|\hat{s}\rangle$ :

$$\langle\hat{s}|\hat{s}\rangle = \int_{>0}^{\infty} dk k \frac{\tilde{q}_s^2(k)}{k^2}, \quad (29)$$

the term after the integration measure is equal to the monochromatic absorption cross section, except for a factor of 4 [see Eq. (33) for the case of spheres]. Most importantly, as long as the frequency components of the illuminating bath are uncorrelated, the rate of absorption of photons and energy in Eq. (6) and Eq. (7), respectively, can be computed using  $|\hat{s}\rangle\langle\hat{s}|$  instead of the non-frequency coupling  $P_s$  defined in Eq. (27), even though  $P_s \neq |\hat{s}\rangle\langle\hat{s}|$  in this case (see App. D). Moreover, the  $|\hat{s}\rangle$  are orthogonal, and their incoming versions are absorbed independently as in Eq. (5), that is:

$$\langle\hat{s}|\hat{u}\rangle = \delta_{su} \langle\hat{s}|\hat{u}\rangle, \text{ and } \langle\hat{s}|Q|\hat{u}\rangle = \delta_{su} \langle\hat{s}|Q|\hat{s}\rangle, \quad (30)$$

which readily follow from the condition

$$\langle\bar{\lambda}\bar{m}\bar{j}p|kjm\lambda\rangle = \delta_{\bar{j}j} \delta_{\bar{m}m} \delta_{\bar{\lambda}\lambda} \delta(p-k)/k, \quad (31)$$

derived in Eq. (A8), and the orthogonality of the  $\tilde{s}(k)$  in Eq. (26).

T

he physical idea behind the use of  $|\hat{s}\rangle$  as the polychromatic absorption and emission modes is connected to the existence of polychromatic internal modes of the object, such as for example, those corresponding to current density distributions characterized by a set of complex frequencies. Each complex frequency gives rise to a resonance on the real frequency axis. What we assume is that each  $|\hat{s}\rangle$  corresponds to one internal mode, which can potentially be excited by a given illumination as long as the spectrum of the illumination has some overlap with the spectrum of  $|\hat{s}\rangle$ . Then, upon relaxation, the modal current density emits photons whose individual spectra are the whole spectrum of  $|s\rangle^{\text{out}} = |\hat{s}\rangle^{\text{out}} / \sqrt{\langle\hat{s}|\hat{s}\rangle^{\text{out}}}$ . Therefore, the emission can contain frequency components that are not present in the illumination albeit always conserving energy. Actually, the model of emission that we put forward can also be applied to model the luminescence of an object upon illumination with a monochromatic continuous wave laser. A monochromatic continuous wave laser is a stationary illumination, and also meets the aforementioned frequency uncorrelation needed for using  $|\hat{s}\rangle$  because the only non-zero cross-correlations among two frequency components happens when the two frequencies are identical to the laser frequency.

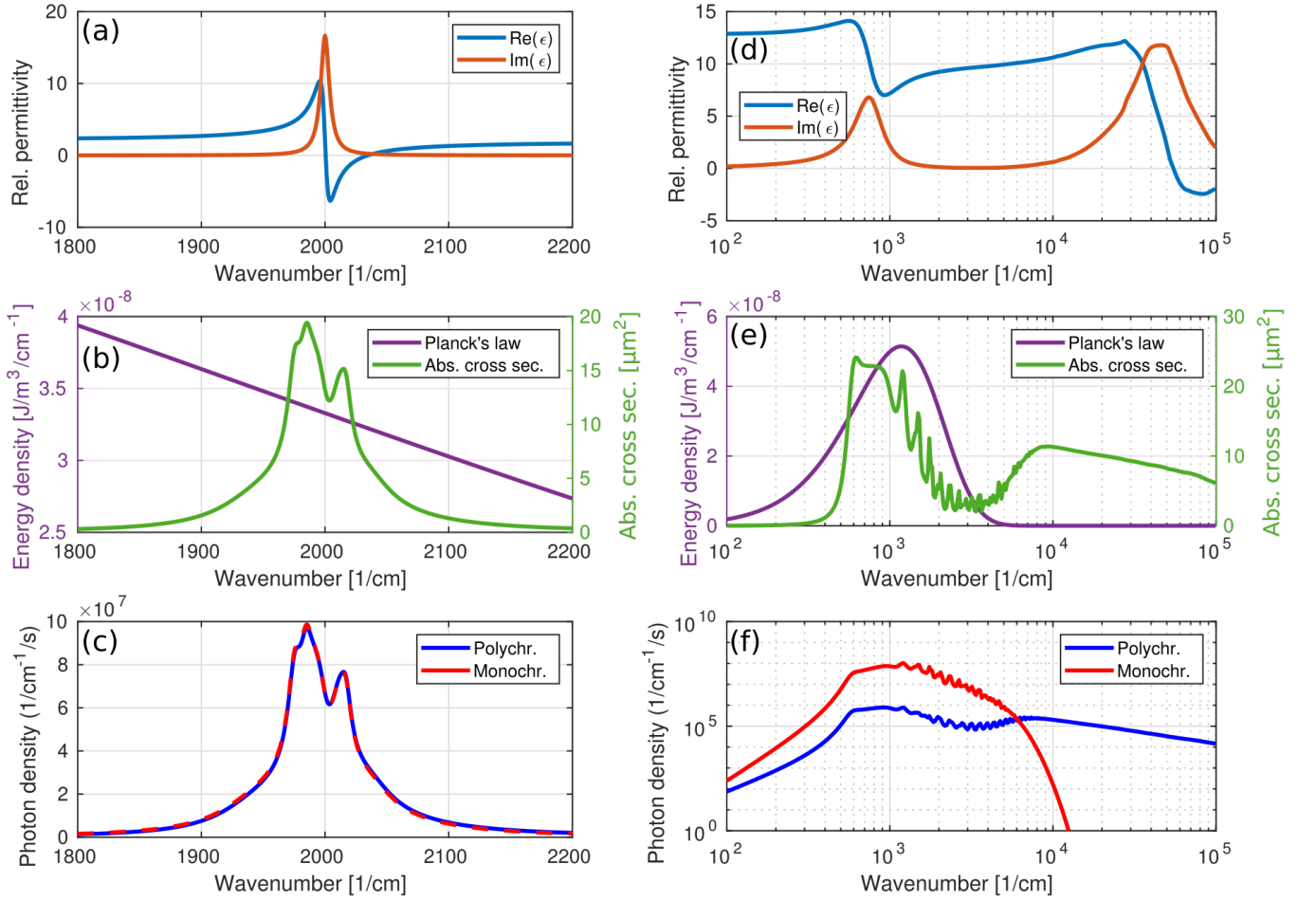


FIG. 2. Thermal spectra of two different spheres, one made of a single-Lorentzian material (first column) and one made of silicon carbide (second column). Each sphere has a  $2\mu\text{m}$  radius. The plots (a) and (d) on the top row show the real and imaginary parts of the relative permittivity of the materials. The plots (b) and (e) on the second row show the absorption cross-section spectra of the spheres, as well as the energy density of the incident Planckian thermal field. The plots (c) and (f) on the third row show the thermal radiation spectra computed in two different ways: the polychromatic method introduced in this article (blue curves), and the common monochromatic method (red curves). The case of a single-Lorentzian material shown in (c) demonstrates that the difference between the two methods tends to disappear when the resonances of the system become very narrow around one central frequency. On the other hand, the case of SiC in (f) shows a substantial difference between the predictions: the usual monochromatic theory predicts a spectrum that is concentrated near the Planckian spectrum, whereas the polychromatic theory predicts that a large part of the absorbed energy is re-emitted at larger frequencies.

### A. Achiral spheres

While the T-matrix of a general object can be obtained numerically [31], the case of a spherically symmetric particle can be treated analytically with Mie theory. We will further assume that the sphere is not chiral. Appendix E contains the derivation of the following expressions.

For the polychromatic approach, the thermal angular

spectrum from Eq. (22) results in:

$$\mathbb{E} \left\{ |\langle \lambda \mathbf{k} | \Phi_{\text{thermal}} \rangle^{\text{out}}|^2 \right\} = \sum_{j=1}^{j_{\text{max}}} \sum_{\tau=\pm 1} \left[ \frac{\int dp p \frac{Ac_0 p^3 (\hbar c_0 p)}{4\pi^2 (\exp(\frac{\hbar c_0 p}{k_B T}) - 1)} \frac{\tilde{q}_{j\tau}^2(p)}{p^2}}{\int dp p (\hbar c_0 p) \frac{\tilde{q}_{j\tau}^2(p)}{p^2}} \right] \frac{2j+1}{8\pi} \frac{\tilde{q}_{j\tau}^2(k)}{k^2}, \quad (32)$$

where  $\tau = 1(-1)$  denotes electric(magnetic) multipoles, and:

$$\begin{aligned} \tilde{q}_{j\tau=1}^2(k) &= -4 \left[ \Re \{a_j(k)\} + |a_j(k)|^2 \right], \\ \tilde{q}_{j\tau=-1}^2(k) &= -4 \left[ \Re \{b_j(k)\} + |b_j(k)|^2 \right], \end{aligned} \quad (33)$$

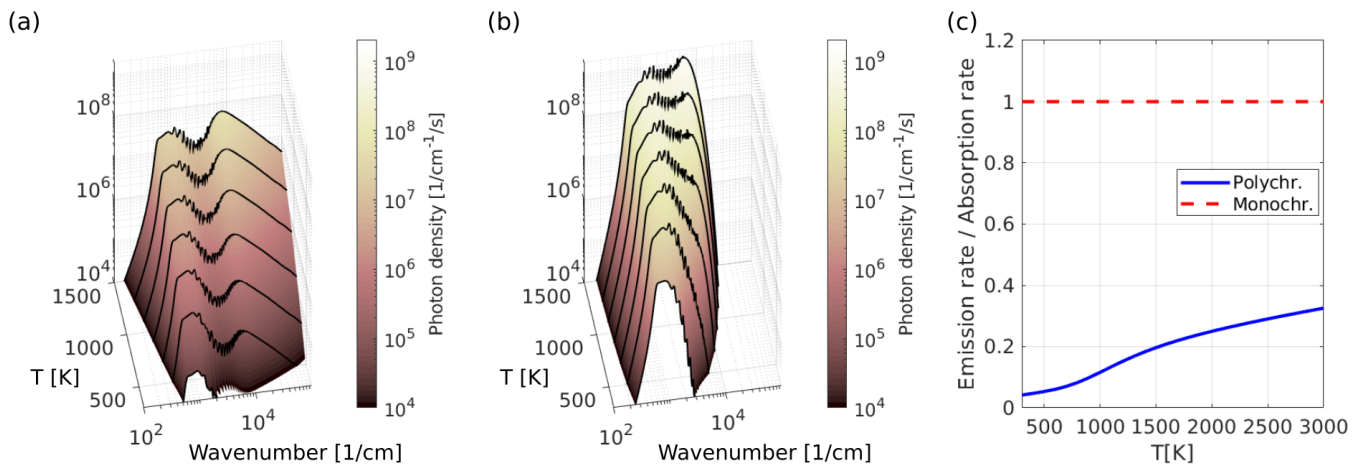


FIG. 3. Temperature dependence of the thermal emission of a SiC sphere. Panels (a) and (b) show the emission spectra predicted by the polychromatic theory of this work and the usual monochromatic theory, respectively; in each plot, the z-scale and the color show the photon density as a function of the wavenumber and temperature. The wavenumber and photon density scales are logarithmic. Panel (c) plots the ratio of the number of emitted photons and the number of absorbed photons.

where  $a_j$  and  $b_j$  are the electric and magnetic Mie coefficients, respectively. Such coefficients can be computed using publicly available codes such as [43] for homogeneous spheres. The package TREAMS has been recently released [36], where the polychromatic T-matrices of homogeneous and multilayered spheres can be easily obtained in the form of the  $\underline{T}(k)$  appearing in Eq. (25).

For the monochromatic approach, Eq. (23) results in:

$$\mathbb{E} \left\{ |\langle \lambda \mathbf{k} | \Phi_{\text{thermal}}^{\text{out}} \rangle|^2 \right\} = \sum_{j=1}^{j_{\text{max}}} \sum_{\tau=\pm 1} \left[ \frac{A_{C_0} k^3}{4\pi^2 \left( \exp\left(\frac{\hbar c_0 k}{k_B T}\right) - 1 \right)} \right] \frac{2j+1}{8\pi} \frac{\tilde{q}_{j\tau}^2(k)}{k^2}. \quad (34)$$

The terms inside the square brackets in Eqs. (32) and (34) determine the difference between the two approaches.

Depending on the object and its material composition, the two approaches can yield either very similar or substantially different thermal emission spectra. In Fig. 2 we consider two examples, each of which is a sphere in air, illuminated by black-body radiation from the environment at temperature 600 K. The first sphere is made of a material that only has a single Lorentzian resonance in its permittivity spectrum [Fig. 2(a)]; in the example we set  $\epsilon = \epsilon_{\text{bg}} + \omega_p^2 / (\omega_0^2 - \omega^2 - i\omega\gamma)$  with  $\epsilon_{\text{bg}} = 2$ ,  $\omega_p = 1 \times 10^{14}$  rad/s,  $\omega_0 = 6 \times 10^{13}$  rad/s, and  $\gamma = 1.59 \times 10^{12}$  rad/s. Consequently, the sphere absorbs only in a narrow bandwidth [green curve in Fig. 2(b)] that is much narrower than the width of the Planckian thermal spectrum (purple curve). In this case, the polychromatic theory of this work and the usual monochromatic theory agree, as expected from App. C [Fig. 2(c) shows the photon density of emission]. The second example is a sphere made of silicon carbide (SiC), a material often utilized in high-temperature applications. As seen from the imaginary part of the permittivity spectrum [red curve

in Fig. 2(d), data taken from [44]], it exhibits high absorption in both far-infrared and near-infrared while being mostly transparent in the mid-infrared around  $2000 \text{ cm}^{-1}$ . This behaviour is reproduced in the absorption cross section of the sphere, which shows it can absorb to a varying extent throughout the spectrum [green curve in Fig. 2(e)]. In this case, the emission spectra predicted by the two theories are quite different, as seen in Fig. 2(f). The monochromatic theory (red curve) predicts a higher photon density around the peak of the Planck spectrum ( $1300 \text{ cm}^{-1}$ ) but a high-frequency tail that falls off rapidly. In contrast, the polychromatic theory (blue curve) predicts a flatter spectrum with a long tail. This tail exhibits an overall  $1/k$  dependence, but we expect it to eventually fall off faster at even larger wavenumbers. This expectation is based on the extension of the refractive index data with a Lorentzian fit, which then results in a  $1/k^3$  dependence of the blue curve, ensuring the convergence of both the radiated number of photons and radiated energy to finite values. The significant difference between the monochromatic and polychromatic predictions should be noticeable in experiments. Nevertheless, the proportion of visible and ultraviolet light from a sphere heated up to 600 K is questionable, and points to a potential inadequacy of the chosen modes. It should be noted, however, that we did not account for the temperature dependence of the optical constants in these calculations.

The difference between the theories inspires us to study the temperature dependence of the emission. Figures 3(a) and (b) show the temperature dependence of the emission spectrum as predicted by the polychromatic and monochromatic theory, respectively. The width of the emission spectrum increases with temperature, but much more noticeably for the monochromatic case. As noted in Fig. 2(f) the spectrum predicted by the poly-

chromatic theory is much wider than the one predicted by the monochromatic theory, and this proves this is the case, possibly until very high temperatures are reached. Finally, we note another interesting but expected difference between the theories. Fig. 3(c) shows the ratio of the number of emitted and the number of absorbed photons per second as a function of temperature. For the monochromatic theory this ratio is always unity, while for the polychromatic theory (which predicts more emission in high frequencies / large photon energies) the ratio is small, but increases with temperature. This is a consequence of energy conservation: If more high-energy photons are emitted, then the emission rate has to be smaller.

## V. DISCUSSION AND OUTLOOK

We have put forward a polychromatic framework to quantitatively predict emission in the stationary regime, that is, when the rates of emission and absorption do not change with time. The framework is based on identifying a set of independent polychromatic absorption modes, and assuming that the emission will occur also independently through the radiating versions of the polychromatic absorption modes. A Kirchhoff-like law is obtained per mode by enforcing that, for each independent channel, the rate of energy absorption is equal to the rate of energy emission. The polychromatic character of the theory endows it with in two inherent properties that are desirable for modeling emission: The emission at frequencies that are not present in the illumination, and the change in the number of photons by emission rates that are higher or lower than the absorption rates.

The computations make use of the T-matrix framework. The many publicly available resources for T-matrix computations [31] together with the formulas in our paper allow one to readily compute quantitative predictions for the emission of objects using both the polychromatic and monochromatic approaches. This will facilitate the experimental testing of the theory.

The choice of the polychromatic modes is a crucial aspect of the method introduced here. We took the polychromatic modes of the absorption operator to be the modes of emission. However, some of the results indicate that this may not be the correct choice. The search for other sets of modes that would resolve the apparent discrepancy between some of the predicted thermal emission spectra and the intuitive expectations constitutes an interesting avenue of future research. We highlight that the salient properties of the polychromatic theory are independent of the choice of polychromatic modes: Namely the emission in frequencies absent in the illumination, the change in the number of photons, and the applicability to both thermal radiation and stationary luminescence processes that are linear with the input intensity.

## ACKNOWLEDGMENTS

M.V. and I.F-C acknowledge funding by the Deutsche Forschungsgemeinschaft (DFG, German Research Foundation) – Project-ID 258734477 – SFB 1173. M.N. acknowledges support by the KIT through the “Virtual Materials Design” (VIRTMAT) project. I.F-C also acknowledges funding and by the Helmholtz Association via the Helmholtz program “Materials Systems Engineering” (MSE).

## Appendix A: Mathematical setting

The set of solutions of Maxwell equations, together with the electromagnetic scalar product [37], form a Hilbert space, which we denote by  $\mathbb{M}$ . The scalar product between two members of  $\mathbb{M}$  can be computed as:

$$\langle f|g\rangle = \sum_{\lambda=\pm 1} \int_{\mathbb{R}^3} \frac{d^3\mathbf{k}}{k} f_{\lambda}^*(\mathbf{k}) g_{\lambda}(\mathbf{k}), \quad (\text{A1})$$

where  $\mathbf{k}$  is the wavevector,  $\lambda$  the polarization handedness, and  $f_{\lambda}(\mathbf{k})$  and  $g_{\lambda}(\mathbf{k})$  are the coefficient functions of the plane wave expansions of  $|f\rangle$  and  $|g\rangle$ , respectively. The scalar product can also be computed as

$$\langle f|g\rangle = \sum_{\lambda=\pm 1} \int_{>0}^{\infty} dk k \sum_{j=1}^{\infty} \sum_{m=-j}^j f_{jm\lambda}^*(k) g_{jm\lambda}(k), \quad (\text{A2})$$

where the  $f_{jm\lambda}(k)$  and  $g_{jm\lambda}(k)$  are the coefficient functions of the expansions in spherical waves, also known as multipolar fields. The form of the expressions (A1) and (A2) is achieved using the conventions in [28], which we include here for reference.

The electric field of a particular solution  $|f\rangle$  is expanded into plane waves of well-defined helicity  $|\mathbf{k}\lambda\rangle$  as:

$$\mathbf{E}(\mathbf{r}, t) = \sum_{\lambda=\pm 1} \int \frac{d^3\mathbf{k}}{k} f_{\lambda}(\mathbf{k}) |\mathbf{k}\lambda\rangle, \quad (\text{A3})$$

and the plane waves are defined as:

$$|\mathbf{k}\lambda\rangle \equiv \sqrt{\frac{c_0\hbar}{\epsilon_0}} \frac{1}{\sqrt{2}} \frac{1}{\sqrt{(2\pi)^3}} k \hat{\mathbf{e}}_{\lambda}(\hat{\mathbf{k}}) \exp(-ikc_0t) \exp(i\mathbf{k} \cdot \mathbf{r}), \quad (\text{A4})$$

where  $c_0$  is the speed of light in vacuum,  $\hbar$  the reduced Planck constant, and  $\epsilon_0$  the permittivity in vacuum. We highlight the factor of  $k = |\mathbf{k}|$  in the definition of the plane waves, which ensures that they transform unitarily under Lorentz transformations, and the factor of  $1/k$  in Eq. (A3), which makes the volume measure  $\frac{d^3\mathbf{k}}{k}$  invariant under transformations in the Poincaré group.

The expansion in multipoles of well-defined helicity reads:

$$\mathbf{E}(\mathbf{r}, t)^{\text{reg/in/out}} \equiv \int_0^\infty dk k \sum_{\lambda=\pm 1} \sum_{j=1}^\infty \sum_{m=-j}^j f_{jm\lambda}(k) |kjm\lambda\rangle^{\text{reg/in/out}}, \quad (\text{A5})$$

and the regular, incoming, and outgoing multipoles  $|kjm\lambda\rangle^{\text{reg/in/out}}$  are defined as:

$$\begin{aligned} |kjm\lambda\rangle^{\text{reg}} &\equiv \mathbf{S}_{jm\lambda}^{\text{reg}}(k, \mathbf{r}, t) = \\ &= -\sqrt{\frac{c_0\hbar}{\epsilon_0}} \frac{1}{\sqrt{2\pi}} k i^j \times \left( \exp(-ikc_0t) \mathbf{N}_{jm}^{\text{reg}}(k|\mathbf{r}|, \hat{\mathbf{r}}) + \lambda \exp(-ikc_0t) \mathbf{M}_{jm}^{\text{reg}}(k|\mathbf{r}|, \hat{\mathbf{r}}) \right), \\ |kjm\lambda\rangle^{\text{in/out}} &\equiv \mathbf{S}_{jm\lambda}^{\text{in/out}}(k, \mathbf{r}, t) = \\ &= -\frac{1}{2} \sqrt{\frac{c_0\hbar}{\epsilon_0}} \frac{1}{\sqrt{2\pi}} k i^j \times \left( \exp(-ikc_0t) \mathbf{N}_{jm}^{\text{in/out}}(k|\mathbf{r}|, \hat{\mathbf{r}}) + \lambda \exp(-ikc_0t) \mathbf{M}_{jm}^{\text{in/out}}(k|\mathbf{r}|, \hat{\mathbf{r}}) \right), \end{aligned} \quad (\text{A6})$$

where the  $\mathbf{M}$  and  $\mathbf{N}$  have the usual definitions (see e.g. [28, Eqs. (50,51)]).

The expansions in Eq. (A3) and Eq. (A5), together with the requirements

$$\langle \bar{\lambda} \bar{m} \bar{j} p | f \rangle = f_{\bar{j} \bar{m} \bar{\lambda}}(p), \quad \text{and} \quad \langle \bar{\lambda} \mathbf{q} | f \rangle = f_{\bar{\lambda}}(\mathbf{q}), \quad (\text{A7})$$

impose the conditions

$$\begin{aligned} \langle \bar{\lambda} \bar{m} \bar{j} p | k j m \lambda \rangle &= \delta_{\bar{j} j} \delta_{\bar{m} m} \delta_{\bar{\lambda} \lambda} \frac{\delta(p-k)}{k}, \quad \text{and} \\ \langle \bar{\lambda} \mathbf{q} | \mathbf{k} \lambda \rangle &= \delta_{\bar{\lambda} \lambda} \delta(\mathbf{k} - \mathbf{q}) k. \end{aligned} \quad (\text{A8})$$

One advantage of using the electromagnetic Hilbert space for the study of light-matter interaction is that the amount of fundamental quantities contained in a given field is easily formulated:  $\langle f | \Gamma | f \rangle$ , where  $\Gamma$  is the self-adjoint operator representing the fundamental quantity, for example energy or momentum. In the multipolar basis, the energy of the field would be computed as:

$$\langle f | H | f \rangle = \sum_{jm\lambda} \int_{>0}^\infty dk k (\hbar c_0 k) |f_{jm\lambda}(k)|^2. \quad (\text{A9})$$

### 1. $\mathbf{Q}$ is compact and hence admits a singular-value decomposition

The scattering operator  $\mathbf{S}$  of a material system acts on incoming fields to produce the corresponding outgoing fields, and it is related to the  $\mathbf{T}$  operator as  $\mathbf{S} = \mathbf{I} + \mathbf{T}$ . We assume that  $\mathbf{T}$  has a finite operator norm:  $|\mathbf{T}| < \infty$ , where the operator norm is the one induced by the scalar product in  $\mathbb{M}$ . The assumption  $|\mathbf{T}| < \infty$  can be seen as

imposing that the coupling strength between the object and the radiation field is finite, which means that all scattering cross-sections are finite. Under such assumption, the  $\mathbf{T}$  operator admits a singular value decomposition, because the assumption  $|\mathbf{T}| < \infty$  implies that  $\mathbf{T}$  is a Hilbert-Schmidt operator, which implies that  $\mathbf{T}$  is compact (see e.g. [45, p. 32], or [46, Sec. 10]). Compact operators are known to have a singular value decomposition (see e.g. [46, Sec. 8], or [45, Sec 15.4]). Given a compact operator  $\mathbf{X}$ , we can expand it as a sum over a discrete index  $s = 1, 2, \dots$

$$\mathbf{X} = \sum_s x_s |u_s\rangle \langle v_s|,$$

where  $x_s$  is a non-increasing series of real and positive numbers  $x_1 \geq x_2 \geq x_3 \geq \dots$  which meets  $x_s \rightarrow 0$  as  $s \rightarrow \infty$ , and the  $|v_s\rangle$  and  $|u_n\rangle$  are complete orthonormal systems for the domain and the range of  $\mathbf{X}$ , respectively.

Since  $\mathbf{T}$  is compact, and the adjoints, sums, and products of compact operators produce compact operators,  $\mathbf{Q}$  is compact, and hence admits a singular value decomposition, written in Eq. (4).

### Appendix B: The value of $\mathbb{E}\{|\psi_\lambda(k)|^2\}$ for a Planckian thermal bath

Before computing it, let us see how  $\mathbb{E}\{|\psi_\lambda(k)|^2\}$  determines the average total number of photons and average

energy in  $|\Psi_{\text{bath}}\rangle^{\text{in}}$ . For the number of photons:

$$\begin{aligned} & \mathbb{E} \left\{ \langle \Psi_{\text{bath}} | \Psi_{\text{bath}} \rangle^{\text{in}} \right\} = \\ & \mathbb{E} \left\{ \sum_{\lambda=\pm 1, \bar{\lambda}=\pm 1} \int_{\mathbb{R}^3} \frac{d^3 \mathbf{k}}{k} \int_{\mathbb{R}^3} \frac{d^3 \mathbf{q}}{q} \psi_{\bar{\lambda}}^*(\mathbf{q}) \psi_{\lambda}(\mathbf{k}) \langle \bar{\lambda} \mathbf{q} | \mathbf{k} \lambda \rangle \right\} \\ & = \sum_{\lambda=\pm 1} \int_{\mathbb{R}^3} \frac{d^3 \mathbf{k}}{k} \mathbb{E} \{ |\psi_{\lambda}(\mathbf{k})|^2 \} = 8\pi \int_{>0}^{\infty} dk k \mathbb{E} \{ |\psi_{+}(k)|^2 \}, \end{aligned} \quad (\text{B1})$$

where the second equality follows from  $\langle \bar{\lambda} \mathbf{q} | \mathbf{k} \lambda \rangle = \delta_{\lambda \bar{\lambda}} \delta(\mathbf{k} - \mathbf{q}) k$ , derived in Eq. (A8), and the third from solving the angular integral using isotropy of the  $\mathbb{E} \{ |\psi_{\lambda}(\mathbf{k})|^2 \}$ , and their equal value for both helicities. Very similar steps results in the expression of the average energy:

$$\mathbb{E} \left\{ \langle \Psi_{\text{bath}} | \mathbf{H} | \Psi_{\text{bath}} \rangle^{\text{in}} \right\} = 8\pi \int_{>0}^{\infty} dk k (\hbar c_0 k) \mathbb{E} \{ |\psi_{+}(k)|^2 \}, \quad (\text{B2})$$

where we have used that  $\mathbf{H} | \mathbf{k} \lambda \rangle = \hbar c_0 k | \mathbf{k} \lambda \rangle$ .

Let us now consider the surface of the smallest sphere that encloses the object in question, and assume that such surface has area  $A$ . The photon flux incoming through the sphere is the same as the incoming photon flux computed on the surface of the object, which is not necessarily spherical. Let us imagine momentarily that there is no object. Then, the power and spectral characteristics of the incoming and outgoing radiation into and out of the sphere are identical. We will assume that the incoming radiation does not change when the object is placed back, and characterize  $|\Psi_{\text{bath}}\rangle^{\text{in}}$  by characterizing the radiation outgoing from a spherical volume with surface area  $A$  which does not contain the object. Such outgoing thermal radiation is described by Planck law. At temperature  $T$ , the energy per second radiated out of the spherical volume is:

$$A \int_{>0}^{\infty} dk \frac{2\hbar c_0^2 k^3}{\pi \left( \exp\left(\frac{\hbar c_0 k}{k_B T}\right) - 1 \right)}, \quad (\text{B3})$$

which is readily reached from the equations in [47, p. 54] by changing the integration variable from the frequency to the wavenumber.

We assume that the energy per second for the incoming field  $|\Psi_{\text{bath}}\rangle^{\text{in}}$  is also equal to Eq. (B3). Having fixed a reference time period  $t_p = 1$ , we may now equate Eq. (B3) and Eq. (B2) to obtain:

$$\mathbb{E} \{ |\psi_{+}(k)|^2 \} = \frac{A c_0 k}{4\pi^2 \left( \exp\left(\frac{\hbar c_0 k}{k_B T}\right) - 1 \right)}. \quad (\text{B4})$$

### Appendix C: Formula for the monochromatic plane wave approach. Agreement with the polychromatic approach of in the narrowband limit.

Assuming reciprocity, the directional Kirchoff law [40, Eq. (2.18)] relates the emissivity in a given direction to the absorptivity of the object in the opposite direction, times the Planck spectrum.

$$\begin{aligned} & \mathbb{E} \left\{ |\langle \lambda \mathbf{k} | \Phi_{\text{thermal}} \rangle^{\text{out}}|^2 \right\} = \\ & P_{\text{abs}}(|-\mathbf{k} \lambda\rangle) \mathbb{E} \left\{ |\langle \lambda - \mathbf{k} | \Psi_{\text{bath}} \rangle^{\text{in}}|^2 \right\}. \end{aligned} \quad (\text{C1})$$

We can make Eq. (C1) more explicit. We know from the isotropy of the Planckian bath and Eq. (B4) that:

$$\begin{aligned} \mathbb{E} \left\{ |\langle \lambda - \mathbf{k} | \Psi_{\text{bath}} \rangle^{\text{in}}|^2 \right\} &= \mathbb{E} \{ |\psi_{\lambda}(-\mathbf{k})|^2 \} = \mathbb{E} \{ |\psi_{+}(k)|^2 \} \\ &= \frac{A c_0 k}{4\pi^2 \left( \exp\left(\frac{\hbar c_0 k}{k_B T}\right) - 1 \right)}. \end{aligned} \quad (\text{C2})$$

Since the probability of absorption is equal to  $k^2 \langle \lambda - \mathbf{k} | \mathbf{Q} | -\mathbf{k} \lambda \rangle$  ([22, Eq. (S43)]), we can write:

$$\begin{aligned} & \mathbb{E} \left\{ |\langle \lambda \mathbf{k} | \Phi_{\text{thermal}} \rangle^{\text{out}}|^2 \right\} = \\ & k^2 \langle \lambda - \mathbf{k} | \mathbf{Q} | -\mathbf{k} \lambda \rangle \frac{A c_0 k}{4\pi^2 \left( \exp\left(\frac{\hbar c_0 k}{k_B T}\right) - 1 \right)} \stackrel{\text{Eq. (4)}}{=} \\ & \sum_s |\langle \lambda - \mathbf{k} | \hat{s} \rangle|^2 \left[ \frac{A c_0 k^3}{4\pi^2 \left( \exp\left(\frac{\hbar c_0 k}{k_B T}\right) - 1 \right)} \right]. \end{aligned} \quad (\text{C3})$$

It is easy to see that Eq. (C3) is at odds with the polychromatic approach proposed in this article, following which the angular spectrum should be obtained as in Eq. (22):

$$\begin{aligned} & \mathbb{E} \left\{ |\langle \lambda \mathbf{k} | \Phi_{\text{thermal}} \rangle^{\text{out}}|^2 \right\} = \sum_s \\ & \frac{\sum_{\bar{\lambda}=\pm 1} \int_{>0}^{\infty} dq \frac{A c_0 q^4 (\hbar c_0 q)}{4\pi^2 \left( \exp\left(\frac{\hbar c_0 q}{k_B T}\right) - 1 \right)} \int d\hat{\mathbf{q}} |\langle \bar{\lambda} \mathbf{q} | s \rangle|^2}{\text{out} \langle s | \mathbf{H} | s \rangle^{\text{out}}} |\langle \lambda \mathbf{k} | \hat{s} \rangle^{\text{out}}|^2. \end{aligned} \quad (\text{C4})$$

#### 1. Convergence of the monochromatic and polychromatic predictions when the linewidth of the absorption modes tends to zero

We now show that the results of Eq. (C4) and Eq. (C3) coincide in the limit where the linewidths of all the  $|s\rangle$  modes tend to zero around the same central frequency.

Let us assume that the modes  $|s\rangle$  are narrowband, and their maximal wavenumber content occurs at a given

wavenumber  $k$ . We may model the plane wave coefficients of an almost monochromatic mode as:

$$\langle \bar{\lambda} \mathbf{q} | s \rangle = \begin{cases} \langle \bar{\lambda} k \hat{\mathbf{q}} | s \rangle, & \text{if } |\mathbf{q}| \in [k - \frac{\Delta k}{2}, k + \frac{\Delta k}{2}] \\ 0, & \text{else} \end{cases} \quad (\text{C5})$$

where  $\Delta k \ll k$ .

The result of Eq. (C4) can be then computed in the limit  $\frac{\Delta k}{k} \rightarrow 0$ . First, we use the unit norm of  $|s\rangle$  to write:

$$\begin{aligned} \langle s | s \rangle = 1 &= \sum_{\bar{\lambda}=\pm 1} \int_{\mathbb{R}^3} \frac{d^3 \mathbf{q}}{q} |\langle \bar{\lambda} \mathbf{q} | s \rangle|^2 \\ &\stackrel{\text{Eq. (C5)}}{=} \sum_{\bar{\lambda}=\pm 1} \int_{k-\frac{\Delta k}{2}}^{k+\frac{\Delta k}{2}} dq q \int d\hat{\mathbf{q}} |\langle \bar{\lambda} k \hat{\mathbf{q}} | s \rangle|^2 \quad (\text{C6}) \\ &= k \Delta k \sum_{\bar{\lambda}=\pm 1} \int d\hat{\mathbf{q}} |\langle \bar{\lambda} k \hat{\mathbf{q}} | s \rangle|^2, \end{aligned}$$

where the fourth equality is the result of taking the limit  $\frac{\Delta k}{k} \rightarrow 0$ . We deduce from Eq. (C6) that

$$\frac{1}{k \Delta k} = \sum_{\bar{\lambda}=\pm 1} \int d\hat{\mathbf{q}} |\langle \bar{\lambda} k \hat{\mathbf{q}} | s \rangle|^2 = \sum_{\bar{\lambda}=\pm 1} \int d\hat{\mathbf{q}} |\langle \bar{\lambda} \mathbf{q} | s \rangle|^2. \quad (\text{C7})$$

The result in Eq. (C7) can be substituted in Eq. (C4), together with the following limit

$$\begin{aligned} \lim_{\frac{\Delta k}{k} \rightarrow 0} \int_{k-\frac{\Delta k}{2}}^{k+\frac{\Delta k}{2}} \frac{dq A c_0 q^4 (\hbar c_0 q)}{4\pi^2 \left( \exp\left(\frac{\hbar c_0 q}{k_B T}\right) - 1 \right)} &= \\ \frac{\Delta k A c_0 k^4 (\hbar c_0 k)}{4\pi^2 \left( \exp\left(\frac{\hbar c_0 k}{k_B T}\right) - 1 \right)}, & \quad (\text{C8}) \end{aligned}$$

and that, in the monochromatic limit  $\text{out} \langle s | \mathbf{H} | s \rangle \text{out} \rightarrow \hbar c_0 k$ , to obtain the limit of Eq. (C4) when all the  $|s\rangle$  modes are monochromatic with wavenumber  $k$ :

$$\begin{aligned} \mathbb{E} \left\{ |\langle \lambda \mathbf{k} | \Phi_{\text{thermal}} \rangle^{\text{out}}|^2 \right\} &= \\ \sum_s |\langle \lambda \mathbf{k} | s \rangle^{\text{out}}|^2 \frac{A c_0 k^3}{4\pi^2 \left( \exp\left(\frac{\hbar c_0 k}{k_B T}\right) - 1 \right)}, & \quad (\text{C9}) \end{aligned}$$

which is shown to be identical to Eq. (C3) by using the following relation between the plane-wave components of the incoming  $|\hat{s}\rangle$  and outgoing  $|\hat{s}\rangle^{\text{out}}$  modes:

$$|\langle \lambda \mathbf{k} | \hat{s} \rangle^{\text{out}}| = |\langle \lambda - \mathbf{k} | \hat{s} \rangle|. \quad (\text{C10})$$

#### Appendix D: Equality of energy and photon absorption rates using $P_s$ or $|\hat{s}\rangle\langle\hat{s}|$

In this appendix we show that, as long as the frequency components of the illuminating bath are uncorrelated, the rate of absorption of photons and energy in

Eq. (6) and Eq. (7), respectively, can be computed using  $|\hat{s}\rangle\langle\hat{s}|$  instead of the non-frequency coupling  $P_s$  defined in Eq. (27), even though  $P_s \neq |\hat{s}\rangle\langle\hat{s}|$  in this case.

We start from the definition of the  $P_s$  operators in Eq. (27):

$$P_s = \sum_{\eta, \bar{\eta}} \int_{>0}^{\infty} dk k |k\eta\rangle \langle \bar{\eta} k | \tilde{q}_s^2(k) [\tilde{s}(k)]_{\eta} [\tilde{s}(k)]_{\bar{\eta}}^*, \quad (\text{D1})$$

where we make the notation more compact by introducing the multi-index labels  $\eta \equiv (jm\lambda)$ , and  $\bar{\eta} \equiv (\bar{j}\bar{m}\bar{\lambda})$ .

We consider for the moment a general illumination

$$|\Psi\rangle = \sum_{\eta} \int_{>0}^{\infty} dk k \psi_{\eta}(k) |k\eta\rangle. \quad (\text{D2})$$

Then, the energy absorption through a given  $P_s$  can be computed as

$$\langle \Psi | \frac{P_s \mathbf{H} + \mathbf{H} P_s}{2} | \Psi \rangle = \langle \Psi | P_s \mathbf{H} | \Psi \rangle, \quad (\text{D3})$$

where the equality follows because  $P_s$  is diagonal in frequency, and hence commutes with  $\mathbf{H}$ .

It readily follows from  $\mathbf{H} |k\eta\rangle = (\hbar c_0 k) |k\eta\rangle$  and Eq. (A8) that

$$\begin{aligned} P_s \mathbf{H} | \Psi \rangle &= \\ \sum_{\eta, \bar{\eta}} \int_{>0}^{\infty} dk k \tilde{q}_s^2(k) [\tilde{s}(k)]_{\eta} [\tilde{s}(k)]_{\bar{\eta}}^* (\hbar c_0 k) \psi_{\bar{\eta}}(k) |k\eta\rangle, & \quad (\text{D4}) \end{aligned}$$

and then, that

$$\begin{aligned} \langle \Psi | P_s \mathbf{H} | \Psi \rangle &= \\ \sum_{\eta, \bar{\eta}} \int_{>0}^{\infty} dk k \tilde{q}_s^2(k) [\tilde{s}(k)]_{\eta} [\tilde{s}(k)]_{\bar{\eta}}^* (\hbar c_0 k) \psi_{\eta}(k)^* \psi_{\bar{\eta}}(k). & \quad (\text{D5}) \end{aligned}$$

We now assume that  $|\Psi\rangle$  is a stationary random illumination, and take the expected value of Eq. (D5)

$$\begin{aligned} \mathbb{E} \{ \langle \Psi | P_s \mathbf{H} | \Psi \rangle \} &= \\ \sum_{\eta, \bar{\eta}} \int_{>0}^{\infty} dk k \tilde{q}_s^2(k) [\tilde{s}(k)]_{\eta} [\tilde{s}(k)]_{\bar{\eta}}^* (\hbar c_0 k) \mathbb{E} \{ \psi_{\eta}(k)^* \psi_{\bar{\eta}}(k) \}. & \quad (\text{D6}) \end{aligned}$$

Let us now consider the operators

$$|\hat{s}\rangle\langle\hat{s}| = \sum_{\eta, \bar{\eta}} \int_{>0}^{\infty} dk k \int_{>0}^{\infty} dp p \hat{s}_{\eta}(k) \hat{s}_{\bar{\eta}}^*(p) |k\eta\rangle \langle \bar{\eta} p|, \quad (\text{D7})$$

where the  $\hat{s}_{\eta}(k)$  are kept general for the moment, and use them to compute energy absorption as:

$$\langle \Psi | \frac{\mathbf{H} |\hat{s}\rangle\langle\hat{s}| + |\hat{s}\rangle\langle\hat{s}| \mathbf{H}}{2} | \Psi \rangle. \quad (\text{D8})$$

The computation of one of its terms can be done in two steps. First:

$$|\hat{s}\rangle\langle\hat{s}|\mathbf{H}|\Psi\rangle = \sum_{\eta,\bar{\eta}} \int_{>0}^{\infty} dk k \hat{s}_{\eta}(k) |k\eta\rangle \int_{>0}^{\infty} dp p \hat{s}_{\bar{\eta}}^*(p) (\hbar c_0 p) \psi_{\bar{\eta}}(p), \quad (\text{D9})$$

and then

$$\langle\Psi|\hat{s}\rangle\langle\hat{s}|\mathbf{H}|\Psi\rangle = \sum_{\eta,\bar{\eta}} \int_{>0}^{\infty} dk k \int_{>0}^{\infty} dp p \hat{s}_{\eta}(k) \hat{s}_{\bar{\eta}}^*(p) (\hbar c_0 p) \psi_{\eta}^*(k) \psi_{\bar{\eta}}(p). \quad (\text{D10})$$

The other term can be computed similarly. The total result after including the expected value reads:

$$\mathbb{E} \left\{ \langle\Psi| \frac{\mathbf{H}|\hat{s}\rangle\langle\hat{s}| + |\hat{s}\rangle\langle\hat{s}|\mathbf{H}}{2} |\Psi\rangle \right\} = \sum_{\eta,\bar{\eta}} \int_{>0}^{\infty} dk k \int_{>0}^{\infty} dp p \hat{s}_{\eta}(k) \hat{s}_{\bar{\eta}}^*(p) \frac{\hbar c_0 (k+p)}{2} \mathbb{E} \{ \psi_{\eta}^*(k) \psi_{\bar{\eta}}(p) \}. \quad (\text{D11})$$

We now assume that the frequency components of the illuminating bath are uncorrelated:

$$\mathbb{E} \{ \psi_{\eta}^*(k) \psi_{\bar{\eta}}(p) \} = \mathbb{E} \{ \psi_{\eta}^*(k) \psi_{\bar{\eta}}(k) \} k \delta(k-p), \quad (\text{D12})$$

where the factor of  $k$  next to the Dirac delta keeps the same units on the left- and right-hand sides of the equation.

After substituting Eq. (D12) onto Eq. (D11):

$$\mathbb{E} \left\{ \langle\Psi| \frac{\mathbf{H}|\hat{s}\rangle\langle\hat{s}| + |\hat{s}\rangle\langle\hat{s}|\mathbf{H}}{2} |\Psi\rangle \right\} = \sum_{\eta,\bar{\eta}} \int_{>0}^{\infty} dk k \hat{s}_{\eta}(k) \hat{s}_{\bar{\eta}}^*(k) k^2 (\hbar c_0 k) \mathbb{E} \{ \psi_{\eta}^*(k) \psi_{\bar{\eta}}(k) \}, \quad (\text{D13})$$

it now becomes clear that our choice

$$\hat{s}_{\eta}(k) = \frac{q_s(k)}{k} [\hat{s}(k)]_{\eta} \quad (\text{D14})$$

makes Eq. (D13) equal to Eq. (D6).

Therefore, for stationary illuminations whose frequency components are uncorrelated, the energy absorption rates of a non-energy coupling object can be computed using  $|\hat{s}\rangle\langle\hat{s}|$  instead of the  $P_s$  in Eq. (D1). The same can be said about the photon absorption rate

$$\mathbb{E} \{ \langle\Psi| P_s |\Psi\rangle \} = \mathbb{E} \{ \langle\Psi| \hat{s}\rangle\langle\hat{s}|\Psi\rangle \}, \quad (\text{D15})$$

which can be readily shown with steps that are parallel to the ones for the energy absorption, the only difference being the absence of the  $(\hbar c_0 k)$  terms.

## Appendix E: Thermal angular spectrum of achiral spheres

In this section, we will derive Eq. (32) and Eq. (34), valid for achiral spherical objects. To such end, we will use the basis of multipoles of well-defined parity, commonly known as electric and magnetic multipoles. Such fields can be obtained from the multipoles of well-defined helicity as:

$$|kjm\tau\rangle = \frac{1}{\sqrt{2}} [|kjm\lambda = +1\rangle + \tau |kjm\lambda = -1\rangle], \quad (\text{E1})$$

where  $\tau = 1$  results in electric multipoles, and  $\tau = -1$  in magnetic multipoles. According to Mie theory, the monochromatic  $\tilde{Q}(k)$  in Eq. (25) are diagonal in the above basis, with elements equal to:

$$\tilde{q}_{j\tau=1}^2(k) = -4 [\Re \{a_j(k)\} + |a_j(k)|^2], \text{ and} \quad (\text{E2})$$

$$\tilde{q}_{j\tau=-1}^2(k) = -4 [\Re \{b_j(k)\} + |b_j(k)|^2],$$

where  $a_j$  and  $b_j$  are the electric and magnetic Mie coefficients, respectively. The spherical symmetry brings about the common  $m$ -th fold degeneracy in the angular momentum label  $m = -j \dots j$ .

The form of the  $|\hat{s}\rangle$  singular modes is readily reached thanks to such degeneracy and diagonal structure:

$$|\hat{s}\rangle = \int_{>0}^{\infty} dk k \frac{\tilde{q}_{j\tau}(k)}{k} |kjm\tau\rangle. \quad (\text{E3})$$

Since each  $s$  denotes a triple  $(jm\tau)$ , we will also use the notation  $|\hat{s}\rangle \rightarrow |jm\tau\rangle$  when convenient.

The projections  $|\langle\lambda\mathbf{k}|\hat{s}\rangle|^2$ , which are needed for computing the thermal angular spectrum in Eq. (22) are:

$$|\langle\lambda\mathbf{k}|jm\tau\rangle^{\text{out}}|^2 = \frac{2j+1}{8\pi} \frac{\tilde{q}_{j\tau}^2(k)}{k^2} |d_{-m\lambda}^j(\theta)|^2, \quad (\text{E4})$$

where  $d_{m\lambda}^j(\theta)$  are small Wigner matrices, as defined in [48, Sec. 4.3], and  $\theta = \arccos(k_z/k)$ . Equation E4 follows from Eq. (C10), [28, Eq. (41)], and Eq. (31).

The following angular integral is also needed in Eq. (22):

$$\sum_{\bar{\lambda}} \int d\hat{\mathbf{p}} |\langle\bar{\lambda}\mathbf{p}|\hat{s}\rangle|^2 = \sum_{\bar{\lambda}} \int d\hat{\mathbf{p}} |\langle\bar{\lambda}\mathbf{p}|jm\tau\rangle|^2 = \frac{\tilde{q}_{j\tau}^2(p)}{p^2}, \quad (\text{E5})$$

where the equality follows because  $\int d\hat{\mathbf{p}} |d_{m\bar{\lambda}}^j(\theta)|^2 = \frac{4\pi}{2j+1}$  (see [48, p. 95, Eq. (6)]), and  $|\langle\bar{\lambda} = +1 \mathbf{p}|jm\tau\rangle|^2 = |\langle\bar{\lambda} = -1 \mathbf{p}|jm\tau\rangle|^2$ .

We can now write Eq. (22) as:

$$\mathbb{E} \{ |\langle\lambda \mathbf{k}|\Phi_{\text{thermal}}\rangle^{\text{out}}|^2 \} = \sum_{jm\tau} \frac{\left[ \int d\mathbf{p} \frac{A c_0 p^4 (\hbar c_0 p)}{4\pi^2 (\exp(\frac{\hbar c_0 p}{k_B T}) - 1)} \frac{\tilde{q}_{j\tau}^2(p)}{p^2} \right]}{\text{out} \langle\hat{s}|\mathbf{H}|\hat{s}\rangle^{\text{out}}} \frac{2j+1}{8\pi} \frac{\tilde{q}_{j\tau}^2(k)}{k^2} |d_{-m\lambda}^j(\theta)|^2. \quad (\text{E6})$$

Finally, we use<sup>3</sup>  $\sum_{m=-j}^{m=j} |d_{m\lambda}^j(\theta)|^2 = 1$ :

$$\mathbb{E} \left\{ |\langle \lambda \mathbf{k} | \Phi_{\text{thermal}} \rangle^{\text{out}}|^2 \right\} = \sum_{j\tau} \left[ \frac{\int dp \frac{Ac_0 p^4 (\hbar c_0 p)}{4\pi^2 \left( \exp\left(\frac{\hbar c_0 p}{k_B T}\right) - 1 \right) p^2} \tilde{q}_{j\tau}^2(p)}{\text{out} \langle \hat{s} | H | \hat{s} \rangle^{\text{out}}} \right] \frac{2j+1}{8\pi} \frac{\tilde{q}_{j\tau}^2(k)}{k^2}, \quad (\text{E7})$$

where the expected isotropy of the radiation is apparent, as there is no remaining dependence on the direction of  $\mathbf{k}$ . We see that Eq. (E7) coincides with Eq. (32) after using that:

$$\text{out} \langle \hat{s} | H | \hat{s} \rangle^{\text{out}} = \int_{>0}^{\infty} dk k (\hbar c_0 k) \frac{\tilde{q}_{j\tau}^2(k)}{k^2}. \quad (\text{E8})$$

With similar steps, Eq. (23) for the monochromatic

approach reads:

$$\mathbb{E} \left\{ |\langle \lambda \mathbf{k} | \Phi_{\text{thermal}} \rangle^{\text{out}}|^2 \right\} = \sum_{j\tau} \frac{Ac_0 k^3}{4\pi^2 \left( \exp\left(\frac{\hbar c_0 k}{k_B T}\right) - 1 \right)} \frac{2j+1}{8\pi} \frac{\tilde{q}_{j\tau}^2(k)}{k^2} |d_{-m\lambda}^j(\theta)|^2, \quad (\text{E9})$$

and hence

$$\mathbb{E} \left\{ |\langle \lambda \mathbf{k} | \Phi_{\text{thermal}} \rangle^{\text{out}}|^2 \right\} = \sum_{j\tau} \frac{Ac_0 k^3}{4\pi^2 \left( \exp\left(\frac{\hbar c_0 k}{k_B T}\right) - 1 \right)} \frac{2j+1}{8\pi} \frac{\tilde{q}_{j\tau}^2(k)}{k^2}, \quad (\text{E10})$$

which is Eq. (34).

- 
- [1] M. Planck, *The theory of heat radiation* (Blakiston, 1914).
- [2] G. Kirchhoff, *Abhandlungen über Emission und Absorption* (Akad. Verlag Ges., 1921).
- [3] H. Baltes (Elsevier, 1976) pp. 1–25.
- [4] C. F. Bohren and D. R. Huffman, *Absorption and scattering of light by small particles*, edited by Wiley, Wiley science paperback series (Wiley, New York, 1983).
- [5] M. Krüger, T. Emig, and M. Kardar, Phys. Rev. Lett. **106**, 210404 (2011).
- [6] Y. Öhman, Nature **192**, 254 (1961).
- [7] J.-J. Greffet, R. Carminati, K. Joulain, J.-P. Mulet, S. Mainguy, and Y. Chen, Nature **416**, 61 (2002).
- [8] J.-J. Greffet and C. Henkel, Contemporary Physics **48**, 183 (2007).
- [9] A. Babuty, K. Joulain, P.-O. Chapuis, J.-J. Greffet, and Y. De Wilde, Phys. Rev. Lett. **110**, 146103 (2013).
- [10] A. Manjavacas, S. Thongrattanasiri, J.-J. Greffet, and F. J. G. de Abajo, Applied Physics Letters **105**, 211102 (2014), <https://pubs.aip.org/aip/apl/article-pdf/doi/10.1063/1.4902429/14303721/211102.1.online.pdf>.
- [11] R. Yu, A. Manjavacas, and F. J. García de Abajo, Nature Communications **8**, 2 (2017).
- [12] M. F. Picardi, K. N. Nimje, and G. T. Papadakis, Journal of Applied Physics **133**, 111101 (2023).
- [13] S. Fan and W. Li, Nature Photonics **16**, 182 (2022).
- [14] X. Li, Z. Ding, L. Kong, X. Fan, Y. Li, J. Zhao, L. Pan, D. S. Wiersma, L. Pattelli, and H. Xu, Mater. Adv. **4**, 804 (2023).
- [15] L. Shen, R. Lou, Y. Park, Y. Guo, E. J. Stallknecht, Y. Xiao, D. Rieder, R. Yang, E. S. Runkle, and X. Yin, Nature Food **2**, 434 (2021).
- [16] J. E. Vázquez-Lozano and I. Liberal, Nature Communications **14**, 4606 (2023).
- [17] M. Pascale and G. T. Papadakis, Phys. Rev. Appl. **19**, 034013 (2023).
- [18] M. Pascale, M. Giteau, and G. T. Papadakis, Applied Physics Letters **122**, 100501 (2023), <https://pubs.aip.org/aip/apl/article-pdf/doi/10.1063/5.0142651/16773700/100501.1.online.pdf>.
- [19] P. C. Waterman, Proc. IEEE **53**, 805 (1965).
- [20] G. Gouesbet, Journal of Quantitative Spectroscopy and Radiative Transfer **230**, 247 (2019).
- [21] M. I. Mishchenko, Journal of Quantitative Spectroscopy and Radiative Transfer **242**, 106692 (2020).
- [22] I. Fernandez-Corbaton, D. Beutel, C. Rockstuhl, A. Pausch, and W. Klopper, ChemPhysChem **21**, 878 (2020).
- [23] B. Zerulla, M. Krstić, D. Beutel, C. Holzer, C. Wöll, C. Rockstuhl, and I. Fernandez-Corbaton, Advanced Materials **34**, 2200350 (2022).
- [24] G. W. Kattawar and M. Eisner, Appl. Opt. **9**, 2685 (1970).
- [25] M. Krüger, G. Bimonte, T. Emig, and M. Kardar, Phys. Rev. B **86**, 115423 (2012).
- [26] D. A. B. Miller, L. Zhu, and S. Fan, Proceedings of the National Academy of Sciences **114**, 4336 (2017).
- [27] B. Peterson and S. Ström, Physical review D **8**, 3661 (1973).
- [28] M. Vavilin and I. Fernandez-Corbaton, JQSRT **314**, 108853 (2024).
- [29] P. Wurfel, Journal of Physics C: Solid State Physics **15**, 3967 (1982).
- [30] J.-J. Greffet, P. Bouchon, G. Bruccoli, and F. m. c. Marquier, Phys. Rev. X **8**, 021008 (2018).
- [31] “Scattport website, <https://scattport.org/index.php/light-scattering-software/t-matrix-codes>.”
- [32] T. Wriedt and J. Hellmers, Journal of Quantitative Spectroscopy and Radiative Transfer **109**, 1536 (2008).
- [33] J. Hellmers and T. Wriedt, Journal of Quantitative Spectroscopy and Radiative Transfer **110**, 1511 (2009).
- [34] N. Stefanou, V. Yannopoulos, and A. Modinos, Comput. Phys. Commun. **132**, 189 (2000).
- [35] M. Nečada and P. Törmä, Communications in Computational Physics **30**, 357 (2021).
- [36] D. Beutel, I. Fernandez-Corbaton, and C. Rockstuhl, Computer Physics Communications **297**, 109076 (2024).

<sup>3</sup> Such property is reached using Eq. (10) in p. 88 and the first expression of Eq. (1) in p. 79 of [48].

- [37] L. Gross, *J. Math. Phys.* **5**, 687 (1964).
- [38] I. Fernandez-Corbaton and C. Rockstuhl, *Phys. Rev. A* **95**, 053829 (2017).
- [39] T. Nieminen, H. Rubinsztein-Dunlop, and N. Heckenberg, *Journal of Quantitative Spectroscopy and Radiative Transfer* **79-80**, 1019 (2003), electromagnetic and Light Scattering by Non-Spherical Particles.
- [40] J. R. Howell, M. P. Mengüç, K. Daun, and R. Siegel, *Thermal radiation heat transfer* (CRC press, Boca Raton, 2020).
- [41] I. Fernandez-Corbaton and M. Vavilin, *Symmetry* **15** (2023), 10.3390/sym15101839.
- [42] R. N. S. Suryadharma, M. Fruhnert, C. Rockstuhl, and I. Fernandez-Corbaton, *Phys. Rev. A* **95**, 053834 (2017).
- [43] C. Mätzler, (2002).
- [44] J. I. Larruquert, A. P. Pérez-Marín, S. García-Cortés, L. R. de Marcos, J. A. Aznárez, and J. A. Méndez, *J. Opt. Soc. Am. A* **28**, 2340 (2011).
- [45] R. Kress, *Linear Integral Equations*, Applied Mathematical Sciences (Springer New York, 2013).
- [46] J. Bell, “The singular value decomposition of compact operators on hilbert spaces,” (2014).
- [47] D. G. Andrews, *An introduction to atmospheric physics* (Cambridge University Press, 2010).
- [48] D. A. Varshalovich, A. N. Moskalev, and V. K. Khersonskii, *Quantum theory of angular momentum* (World Scientific: Singapore, 1988).